Progress in PHOTOVOLTAICS

PROGRESS IN PHOTOVOLTAICS: RESEARCH AND APPLICATIONS
Prog. Photovolt: Res. Appl. 2014; **22**:227–241
Published online 25 June 2012 in Wiley Online Library (wileyonlinelibrary.com). DOI: 10.1002/pip.2243

APPLICATION

A low-cost photovoltaic emulator for static and dynamic evaluation of photovoltaic power converters and facilities

Raúl González-Medina*, Iván Patrao, Gabriel Garcerá and Emilio Figueres

Grupo de Sistemas Electrónicos Industriales del Departamento de Ingeniería Electrónica, Universidad Politécnica de Valencia, Camino de Vera s/n, 46022 Valencia, Valencia, Spain

ABSTRACT

In testing maximum power point tracking (MPPT) algorithms running on electronic power converters for photovoltaic (PV) applications, either a PV energy source (PV module or PV array) or a PV emulator is required. With a PV emulator, it is possible to control the testing conditions with accuracy so that it is the preferred option. The PV source is modeled as a current source; thus, the emulator has to work as a current source dependent on its output voltage. The proposed emulator is a buck converter with an average current mode control loop, which allows testing the static and dynamic performance of PV facilities up to 3 kW. To validate the concept, the emulator is used to evaluate the MPPT algorithm of a 230-W experimental microinverter working from a single PV module. Copyright © 2012 John Wiley & Sons, Ltd.

KEYWORDS

photovoltaic emulator; photovoltaic simulator; MPPT testing; photovoltaic inverter

***Correspondence**

Raúl González-Medina, Grupo de Sistemas Electrónicos Industriales del Departamento de Ingeniería Electrónica, Universidad Politécnica de Valencia, Camino de Vera s/n, 46022 Valencia, Spain.

E-mail: raugonme@upvnet.upv.es

Received 20 January 2012; Revised 30 March 2012; Accepted 23 April 2012

1. INTRODUCTION

Every electronic power converter for photovoltaic (PV) applications must be tested under realistic operating conditions because a PV energy source presents a particular relationship between its output voltage and current. Testing of the power converter with varying characteristics of the PV source is very important as it is part of the validation of the final product [1–3].

When testing a PV power converter, there are two options, to test the converter with a real PV energy source (either a PV module or an array of PV modules) or to test it with a PV emulator. When using a real PV source, it is necessary to have a wide space in the testing facility, especially at high power. Besides, it is difficult to set the testing conditions because of the weather dependency. Furthermore, it is necessary to acquire the meteorological conditions (irradiance and temperature) [4], which is expensive and difficult, although they can vary during the test [5,6].

When using a PV emulator, it is easy to set the testing conditions with accuracy, whereas the testing equipment requires a smaller space and cost. Besides, it is very easy to change the test conditions (number and connection of the PV modules, irradiance, temperature, *I–V* characteristic curve, among others), regardless of the weather conditions [7].

Power inverters for PV applications have been evolving to include lower power converters. A few years ago, the most common converters were the central inverters [8], with a power level higher than 50 kW. At present, the most common inverters are the string inverters [8], with a few kilowatts power (2–10 kW). Nowadays, the microinverters are an emerging technology gaining an increasing interest because of their modularity and the possibility of single module maximum power point tracking (MPPT) [9]. A microinverter is a grid-connected inverter operating from a single PV module, working from a low input voltage (<50 V) and providing an output power up to 300 W.

Commercial PV emulators present several drawbacks, as a high cost and the impossibility of emulating rapidly changing atmospheric conditions [6]. In this paper, a low-cost PV emulator based on a buck (direct current–direct current) DC–DC converter [10] and a current–voltage lookup

table is proposed. The emulator is able to simulate the current–voltage curve of a PV source of 3 kW maximum output power. It can be used to test the performance of inverters in PV applications.

A switched mode buck DC–DC converter is a good solution for a low-cost emulator as its worst case efficiency is around 90%, resulting in a low-cost thermal design and a small volume. Linear topologies present a much lower efficiency (35% in some cases), leading to a bulky converter and an expensive thermal design.

A prototype of the proposed emulator has been designed and tested and connected to a PV microinverter to evaluate its performance.

2. PHOTOVOLTAIC SOURCE MODEL

A PV source consists of the series interconnection of several PV cells, which convert the solar radiation to electrical energy. The produced electrical energy is affected by the irradiance level and the temperature of the cell. Each cell has a nonlinear electrical characteristic *I–V* curve [11], and the association of cells (or modules) yields a characteristic curve strongly affected by the most shaded one [12].

It is possible to obtain an equation of the characteristic *I–V* curve by using the mathematical model presented in [13,14]. However, manufacturers of PV sources, instead of the current–voltage parameters of the equation, provide experimental data of the *I–V* curves with irradiance and temperature as running parameters. For this reason, the PV emulator described in this paper uses a lookup table to model the PV source.

In grid-connected applications, the most common PV modules provide around 220 W power at their maximum power point (MPP) at an irradiance level of 1000 W/m^2 and a temperature of 25 °C. The typical *I–V* and *P–V* (power–voltage) curves of one of these modules are shown in Figure 1 (a commercial SLK60P6L module by Siliken S.A.). For a given irradiance level and temperature, there is a characteristic relationship between the output voltage and the current generated. Thus, the behavior of a PV source can be emulated by means of a current source controlled by its output voltage [15].

In Figure 1, the relationship between irradiance and the parameters of the curve can be observed: short-circuit current is strongly affected, the open-circuit voltage is slightly affected, and both the MPP voltage and power vary with the irradiance. This variation justifies the importance of the

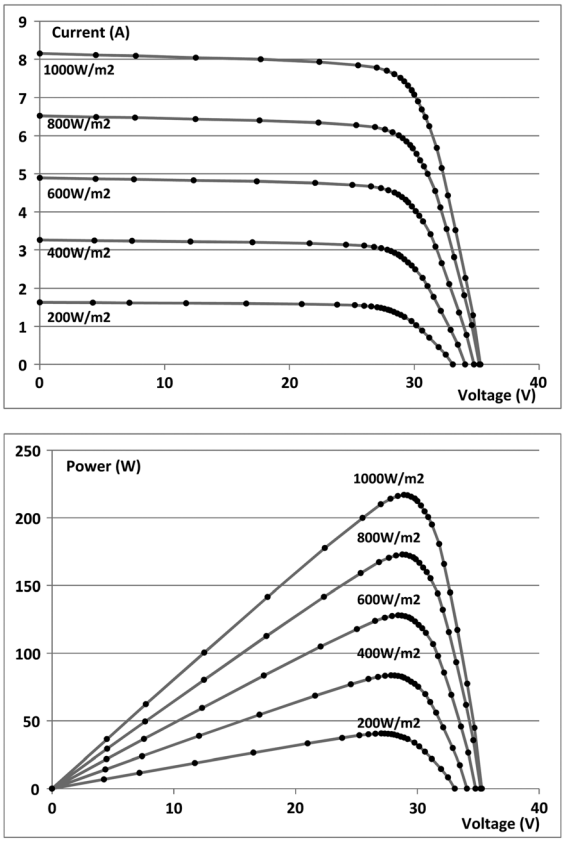

Figure 1. *I–V* and *P–V* characteristics of a commercial SLK60P6L PV module and its dependency of the irradiance. The ambient temperature is 25 °C.

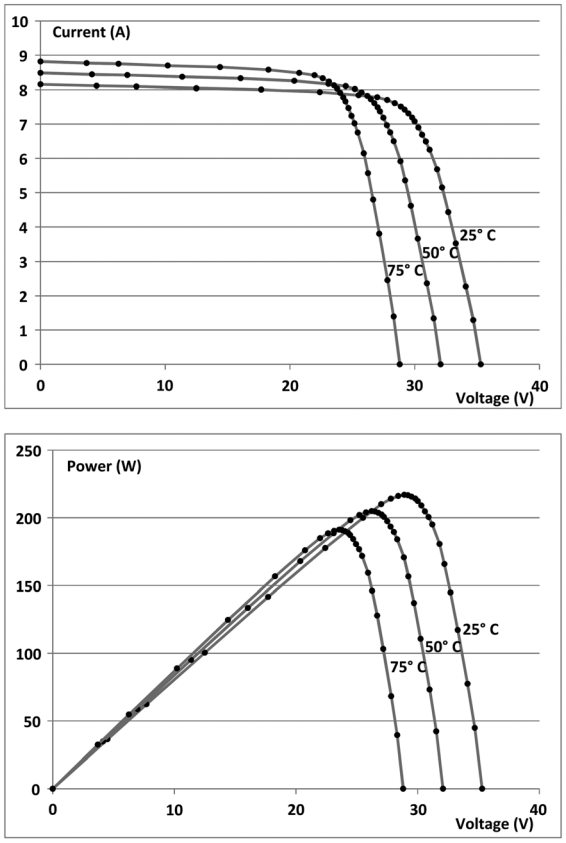

Figure 2. *I–V* and *P–V* characteristics of a commercial SLK60P6L PV module and its dependency of temperature. The irradiance level is 1000 W/m^2.

DOI: 10.1002/pip

MPPT algorithm, ensuring that the inverter tracks the MPP in any climatic condition.

In addition to the irradiance, the temperature also affects the performance of the PV source. The variation of the *I–V* and *P–V* curves with temperature for an irradiance level of 1000 W/m^2 is shown in Figure 2. It can be observed how a higher temperature reduces both the maximum available power and the MPP voltage.

3. PHOTOVOLTAIC EMULATOR

In PV inverters, it is important to obtain a high accuracy from the MPPT algorithm to reach the MPP of the PV source as it strongly affects the overall power generation of the PV installation. The MPPT algorithm is responsible for searching the MPP and keeping the inverter working at this point under all operating conditions such as different irradiance levels and temperature [16].

When researching about MPPT methods, it is mandatory to have a reliable PV emulator that assures the repeatability of the results, capable of simulating all the possible climatic conditions (variations of irradiance and temperature) [17]. However, commercial emulators have a high economic cost [7]. For instance, an Agilent solar array emulator of 60 V/8 A (E4350B) has a cost about $10,000, whereas its output range is quite limited.

Most advanced emulators incorporate a microcontroller and provide to the user the possibility of introducing the *I–V* curve of a PV source at several irradiance levels. It is also possible to emulate the evolution of a PV generator during a long period (1 day, for example) if the software allows to program the evolution of irradiance and temperature during this period.

The PV emulator proposed in this paper can simulate the behavior of PV power source with an open-circuit voltage of 500 V (maximum voltage) and a short-circuit current of 9 A (maximum current), with a power limitation of 3000 W. As the proposed emulator is based on a microcontroller, it can emulate the evolution of the panel *I–V* curve for a long period. An important objective of the proposal is to obtain a low-cost emulator.

In the proposed PV emulator, a 26-point lookup table is created to model the PV source. The lookup table is organized according to voltage values with a higher density of points around the MPP and in the open-circuit zone than

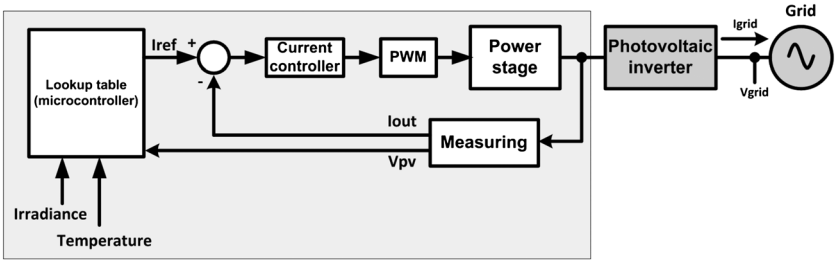

Figure 3. Block diagram of the proposed emulator feeding a grid-connected photovoltaic (PV) inverter. PWM, pulse-width modulation.

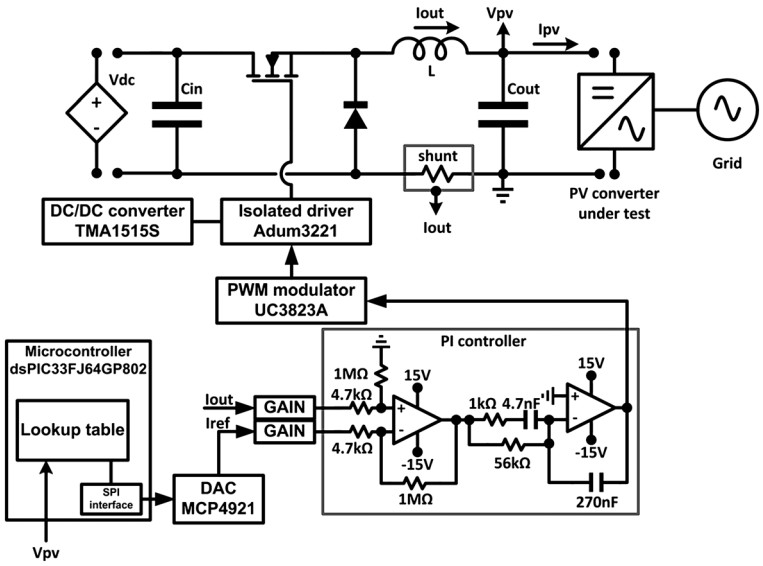

Figure 4. Simplified electronic scheme of the photovoltaic (PV) emulator based on a buck converter feeding a grid-connected micro-inverter. PWM, pulse-width modulation; DAC, digital-to-analog converter.

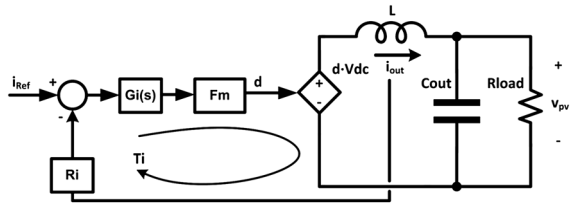

Figure 5. Average mode current control loop of the buck.

in the constant current zone. This strategy provides a great resolution with a short table. The type of the interpolation implemented between adjacent points is linear because it provides enough accuracy with a low computational cost. The points stored in the table can be observed in Figures 1 and 2 (black dots).

A block diagram of the proposed emulator is shown in Figure 3. The power stage acts as a current source dependent on its output voltage, being both magnitudes related by means of the *I–V* curves stored as lookup tables. A lookup table stores the *I–V* curve to be emulated and generates the reference value of the output current. The irradiance and temperature parameters affect the generated curve. A microcontroller allows to recalculate the *I–V* curve "on the fly" to emulate the transient behavior of a PV source. The points belonging to each new *I–V* curve are updated at 5 kHz. This is carried out by means of interpolation along the stored curves, corresponding to different irradiance and temperature levels. The current controller ensures the tracking of the reference value for this current. Because a PV source acts as a current source, it is not necessary to implement a voltage control loop; the lookup table is enough.

The topology used for the power stage is a buck DC–DC converter [18] because it is simple and reliable. As it is a switching converter, the power losses will be low, whereas the converter will have a low size and cost. To supply the buck power stage, it is necessary to use a DC power source with a voltage higher than the open-circuit voltage of the PV source being emulated.

To achieve a crossover frequency of 10 kHz, a 10 times higher (100 kHz) switching frequency has been chosen. This is a usual criterion when implementing a linear control of buck DC–DC converters because the linear small-signal models of switching converters are only valid up to half the switching frequency [20]. Besides, if the switching noise is pushed to 100 kHz, a loop with a 10-kHz crossover frequency is not greatly affected by the switching noise.

Table I. Summary of transfer functions of continuous conduction mode (CCM) buck direct current-direct current (DC-DC) converter with average current control (ACC).

PWM modulator gain	$F_m = \frac{1}{V_{pp}}$
Duty cycle-to-inductor current response	$\frac{i_{out}}{d}(s) = \frac{V_{DC}\cdot(R_{LOAD}\cdot(C_{out}+C_{DC-link})\cdot s+1)}{R_{LOAD}\cdot(L\cdot(C_{out}+C_{DC-link})\cdot s^2+1)+L\cdot s}$
Current-loop regulator	$G_i(s) = \frac{w_i}{s}\cdot\frac{1+\frac{s}{w_z}}{1+\frac{s}{w_p}}$
Current-loop gain	$T_i(s) = \frac{i_{out}}{d}(s)\cdot F_m\cdot R_i\cdot G_i(s)$

PWM, pulse-width modulation.

By taking the switching frequency into account, the chosen power transistor for the buck converter is a metal oxide semiconductor field-effect transistor (MOSFET) because other transistors such as insulated gate bipolar transistors present high switching power losses above 50 kHz and at 520 V input voltage. A crossover frequency of 10 kHz ensures that the emulator is much faster than the PV inverter under test (i.e., much faster than the inverter MPPT algorithm) so that the inverter "sees" the emulator as a real PV source. The crossover frequency of the inverter voltage control loop is usually in the range 1–20 Hz. Thus, the dynamics of the current controller of the PV source emulator does not affect the dynamics of the inverter under test.

To achieve a small size and a low cost of the PV emulator, a buck DC–DC converter running at 100 kHz with a single stage inductor–capacitor (LC) filter is proposed, with a control crossover frequency of 10 kHz. The problems of using low switching frequencies are the need of big output filters, such as the double stage LC filter proposed in [15], and that the control bandwidth is limited so that a good dynamic response is difficult to obtain. The need of big filters is not only a size problem but also a price problem. The proposed buck DC–DC converter uses a single stage LC filter, resulting in a small size and a low cost as it will be shown later. The value of the filter capacitor is very small compared with the typical DC-link input capacitance of PV inverters connected to the emulator so that the inverter dynamics is not affected by this small and unexpensive capacitor. This capacitor is necessary to reduce the switching ripple from the emulator output voltage in applications that do not provide an input capacitance as the test of an emulated PV source loaded by a resistive load. The software-emulated *I–V* characteristic proposed in this paper provides a high flexibility to set the irradiance and temperature of the PV source being emulated.

A simplified electronic scheme of the PV emulator proposed in this paper is shown in Figure 4. In this figure, the emulator is feeding a grid-connected PV inverter. A low-cost microcontroller (Microchip dsPIC33FJ64GP802) senses the output voltage and searches in the chosen *I–V* curve the corresponding reference value of the output current stored in a lookup table. This current reference value is provided to the proportional-integral (PI) current controller through a digital-to-analog converter (DAC). The analog PI controller ensures the tracking of the current reference value with a closed loop bandwidth around 10 kHz. This control

Table II. Value of w_i for different input voltage values.

Number of PV modules being emulated	V_{DC} (volts)	w_i
1	60	13.2
2	120	6.6
≤4	240	3.3
≤8	400	1.98
≤14	540	1.47

PV, photovoltaic.

DOI: 10.1002/pip

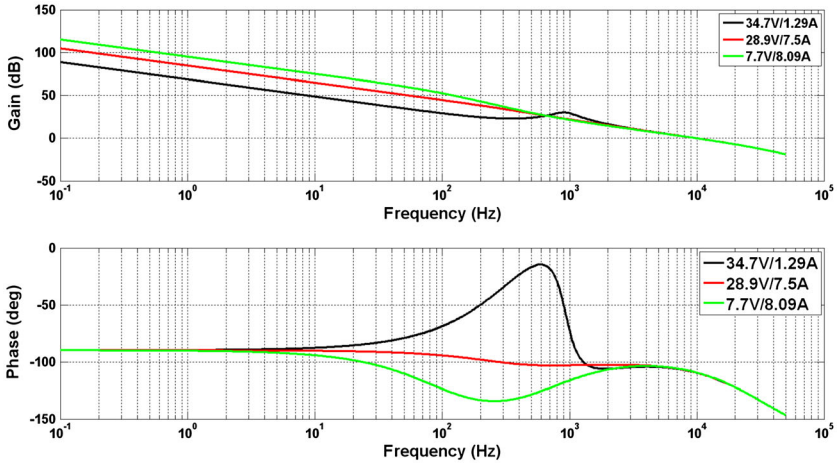

Figure 6. Bode plots of the current-loop gain, $T_i(s)$, for different values of the output voltage V_{PV}. UP: gain, dB. LOW: phase, deg.

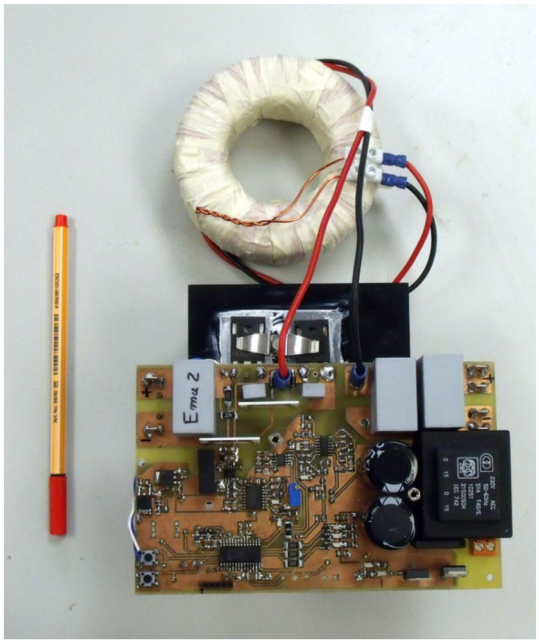

Figure 7. Photovoltaic source emulator.

scheme corresponds to average current mode control [19]. The pulse-width modulation (PWM) modulator adjusts the duty cycle of the buck MOSFET transistor. An isolated driver provides the isolation required between the control circuitry and the MOSFET.

To achieve a crossover frequency as high as 10 kHz, a 10 times higher sampling frequency (100 kHz) is needed in practice. Because it is difficult to run a digital controller at a sampling frequency of 100 kHz with a low-cost microcontroller, the PI controller is implemented by means of operational amplifiers.

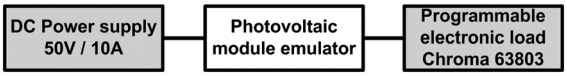

Figure 8. Experimental setup. DC, direct current.

Instead of sensing the current provided to the PV converter under test, the current through the buck converter output inductor (which agrees with the shunt current) is sensed because the latter allows the implementation of average current mode control. It is worth pointing out that the current provided to the PV converter, I_{PV}, has the same average value as the current through the buck inductor, I_{out}, so that by controlling I_{out}, the current I_{PV} is indirectly controlled. The values of the components of the buck circuit are $L = 1.87$ mH, $C_{out} = 16$ µF, $C_{in} = 8$ µF. The emulator is capable of providing an output voltage V_{out} from 10 to 490 V with a maximum output power of 3000 W. The overall cost of the implemented prototype is about $210, having performed the purchase of the electronic components on a small-scale basis. At an industrial manufacturing scale, the production cost would be much lower. As the DC power source is not a part of the emulator, it is not included in the prototype cost.

The block diagram of the current control loop is shown in Figure 5, where $G_i(s)$ is the transfer function of the current controller, F_m is the PWM modulator gain, and R_i is the current sensing gain. The open loop gain of the current loop, $T_i(s)$, is also shown in Figure 5. The dynamic model of the current loop is explained in [20].

The mathematical model of the power stage of the buck converter and all the transfer functions used to adjust the control loop are summarized in Table I, where F_m is the gain of the PWM modulator ($F_m = 0.56\ V^{-1}$), and R_i is the current sensing gain ($R_i = 0.02\ \Omega$). R_{LOAD} is calculated according to the voltage and power delivered to the PV converter under test: $R_{LOAD} = V_{PV}^2/P_{PV}$. In the transfer function of the current controller, $G_i(s)$, w_i is the integrator gain and w_z and w_p are the zero and pole (in rad/s), respectively.

It can be observed that the value of the DC-link capacitance (C_{DC}-link) of the converter connected to the emulator has taken into account in the duty cycle-to-inductor current response (Table I). However, the zero $1/(R_{LOAD}\cdot$

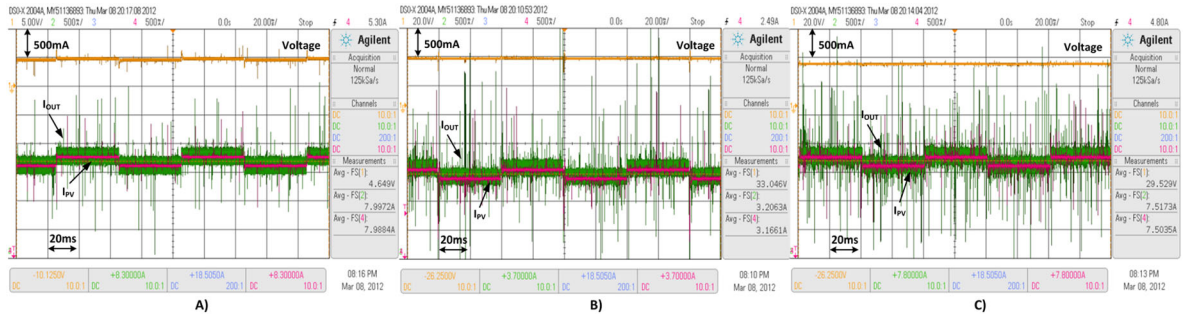

Figure 9. Time domain current and voltage waveforms of the buck converter. (A) High current–low voltage, 8 A/4.7 V. (B) Low current–high voltage, 3.2 A/33 V. (C) High current–high voltage, 7.5 A/29.5 V.

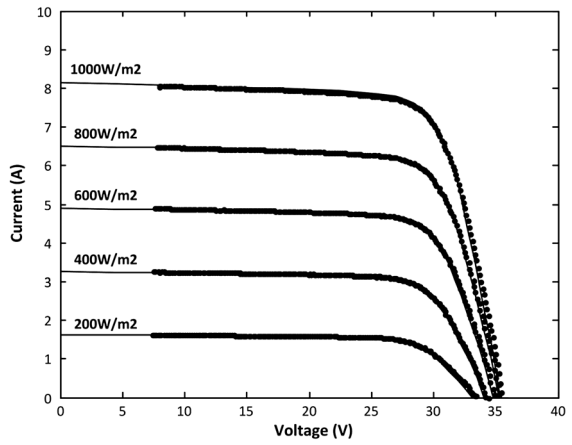

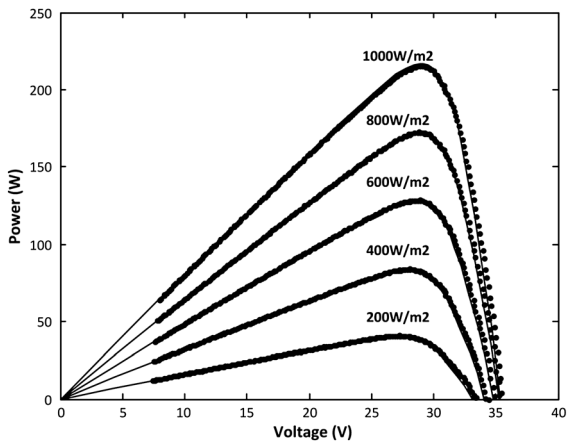

Figure 10. Model (lines) and experimental (dots) *I–V* and *P–V* curves of the emulator at different irradiance levels. The emulated ambient temperature is 25 °C.

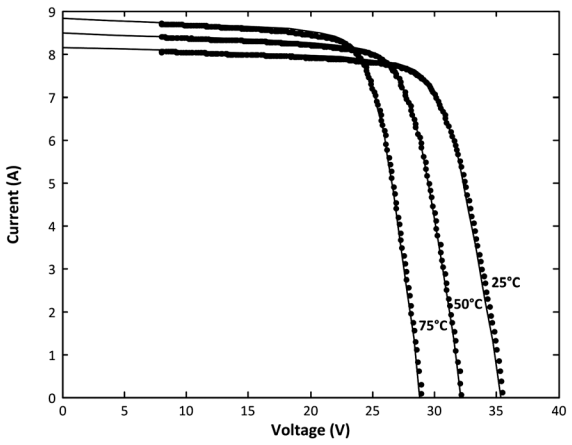

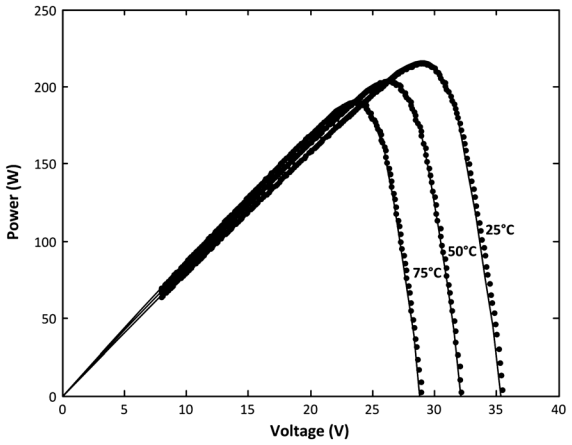

Figure 11. Model (lines) and experimental (dots) *I–V* and *P–V* curves of the emulator at different temperatures. The emulated irradiance is 1000 W/m^2.

($C_{out} + C_{DC\text{-}link}$)) does not significantly affect this transfer function in the medium frequency range, near the crossover frequency. So, the stability is guaranteed over large variations of $C_{DC\text{-}link}$.

It is necessary to adjust the sensing gain ($\underline{R}_i$) of the PV source emulator to adjust the DAC to the output voltage range to obtain the maximum resolution. The adjustment of the sensing gain is carried out by means of a digital potentiometer.

The input voltage value (V_{DC}) can be adjusted to be compatible with different laboratory power supplies. Because the current-loop open loop gain, $T_i(s)$, is strongly affected by the input voltage (V_{DC}), the parameter w_i of the current regulator needs to be automatically adjusted

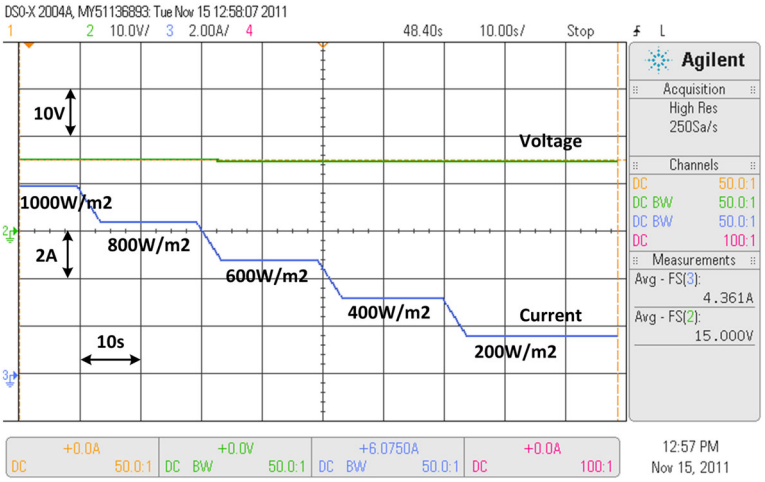

Figure 12. Irradiance steps at a constant voltage: constant current region (15 V).

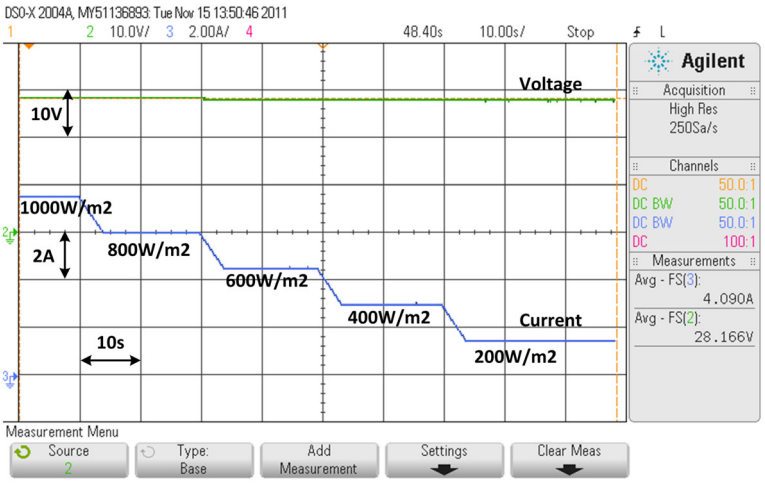

Figure 13. Irradiance steps at a constant voltage: near the maximum power point (28 V).

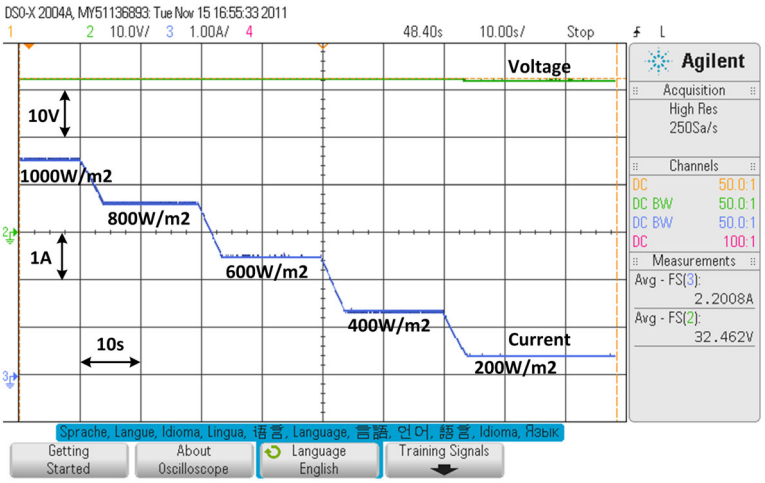

Figure 14. Irradiance steps at constant voltage: constant voltage region (32 V).

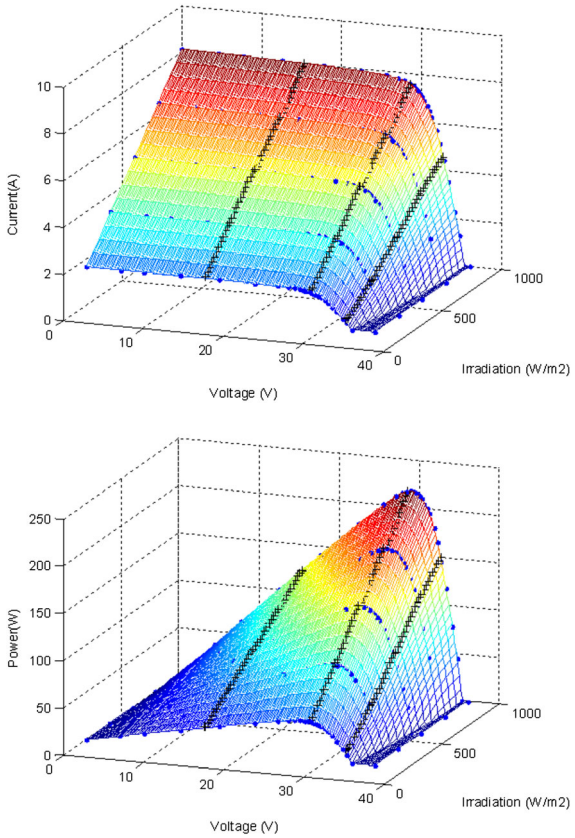

Figure 15. Curves of the emulated photovoltaic module (surface) and experimental data (dots) at irradiance steps.

(by means of the microncontroller) for each different configuration of the emulator. In the experimental results of this paper, the emulator is configured as a single PV module ($V_{DC} = 60$ V, $P_{max} = 220$ W). The current controller is adjusted to obtain a crossover frequency of the current-loop open loop gain, $T_i(s)$, around 10 kHz for any value of V_{DC}, thus having a much higher bandwidth than the voltage loop of PV inverters (which is about 5–20 Hz). The high bandwidth of the PV emulator "seen" by the PV converter under test allows a reliable evaluation of the PV system under dynamic conditions. When the single PV module is being emulated with $V_{DC} = 60$ V, the adjustment values of the current regulator are $w_i = 13.2$ rad/s, $w_z = 3.7$ rad/s, and $w_p = 212.8$ rad/s. For other values of V_{DC}, the value of w_i varies in indirect proportion to V_{DC}, whereas the values of w_z and w_p are kept constant. The values of V_{DC} and w_i programmed are shown in Table II.

Table III. Double stage (DC–DC + DC–AC) microinverter characteristics.

MPP input voltage range (V_{PV_MPP})	24–35Vdc
Input current (I_{PV_MPP})	8 A (max)
Output power	230 W (max)
Switching frequency (DC/DC)	24 kHz
Switching frequency (DC/AC)	10 kHz
Nominal grid	230 V/50 Hz

DC, direct current; AC, alternating current.

The Bode plot of the transfer function $T_i(s)$ is used to adjust the current controller. The stability of the system is guaranteed if the following criteria are achieved: the crossover frequency (gain = 0 dB) is below half the switching frequency, the phase margin (difference between −180 deg and phase at the crossover frequency) is higher than 45 deg and the gain margin 5 dB (the attenuation when the phase is −180 deg and −5 dB). The Bode plots of $T_i(s)$ for the whole output voltage range are depicted in Figure 6. It is observed that the values of the crossover frequency (10 kHz) and the stability margins (phase margin = 70.5 deg, gain margin > 20 dB) are kept in the whole range.

4. EXPERIMENTAL RESULTS

A prototype of the proposed PV emulator on the basis of a buck converter has been designed and implemented for evaluating its performance. A photograph of the prototype is shown in Figure 7. The emulator can reproduce the behavior of a single PV source under different irradiance levels and temperatures, with a maximum output power of 3000 W. To validate the emulator, the behavior a single PV module of 220 W under different irradiance levels and temperatures has been tested.

The *I–V* of the PV source curves has been stored in a lookup table inside the microcontroller. The DAC senses the output voltage and, taking into account the preprogrammed irradiance level and temperature, sets the current reference using the corresponding *I–V* lookup table. Steps in the reference current are avoided using linear interpolation between points of the lookup table.

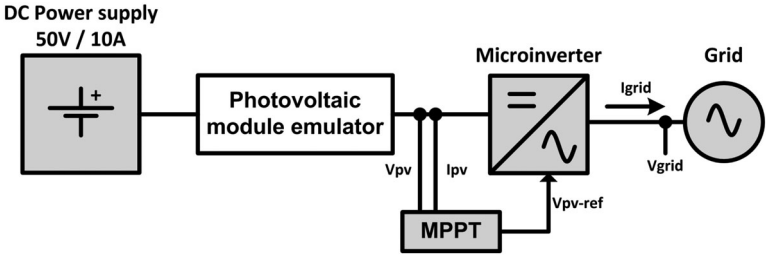

Figure 16. Experimental setup. DC, direct current; MPPT, maximum power point tracking.

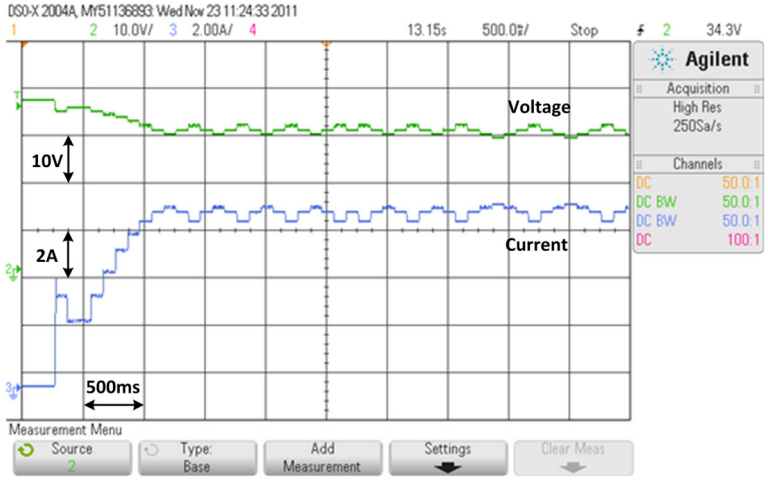

Figure 17. Maximum power point tracking algorithm (1000 W/m^2, 25 °C).

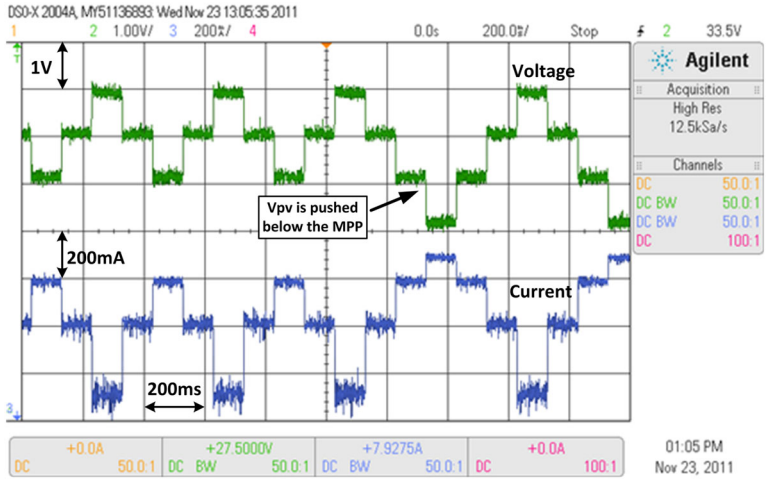

Figure 18. Detail of the voltage and current steps around the maximum power point (MPP) produced by the microinverter maximum power point tracking algorithm. (1000 W/m^2, 25 °C).

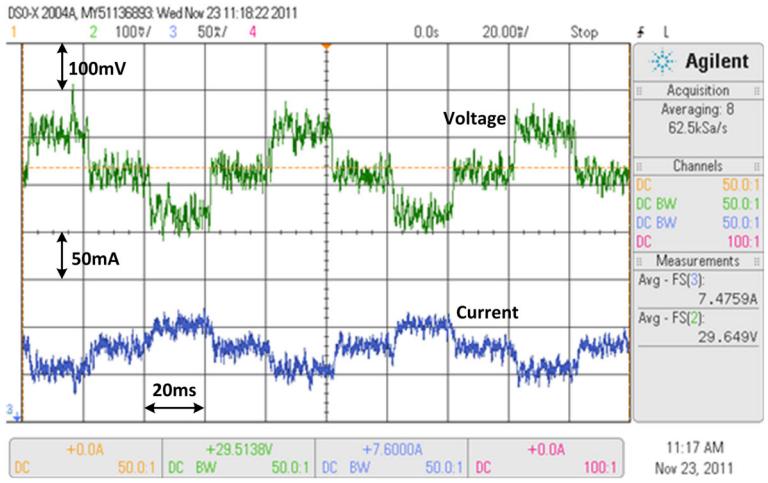

Figure 19. Detail of the voltage and current steps around the maximum power point produced by the microinverter maximum power point tracking algorithm working with 100 mV voltage steps (1000 W/m^2, 25 °C).

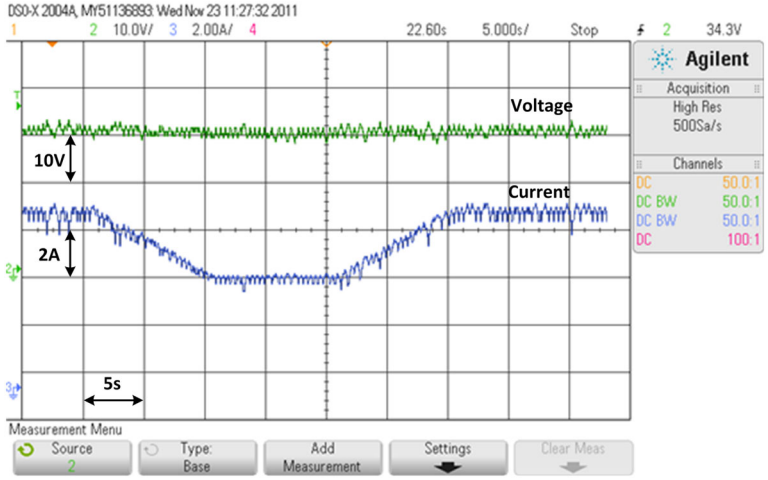

Figure 20. Maximum power point tracking evolution under irradiance steps from 1000 to 600 W/m^2 and back to 1000 W/m^2. Transition time is 10 s. The ambient temperature is 25 °C.

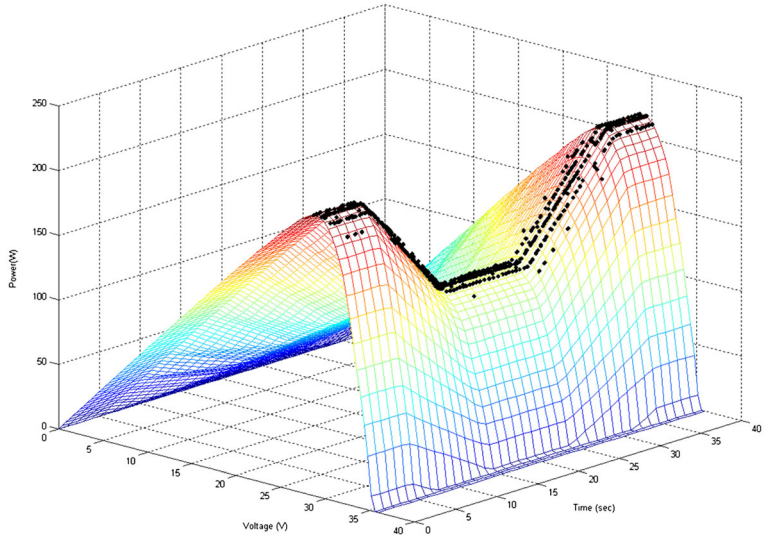

Figure 21. Irradiance steps from 1000 to 600 W/m^2 and back to 1000 W/m^2 plotted over the power–voltage surface. Transition time is 10 s. The ambient temperature is 25 °C. Dots represent the maximum power point tracking evolution.

The experimental setup to test the static characteristics of the PV source emulator is depicted in Figure 8. The prototype is connected to a programmable electronic load (CHROMA model 63803). The electronic load is configured in constant voltage mode, emulating an inverter voltage control loop, which regulates the output voltage of the PV emulator. The emulator is powered from an external power source of 60 V_{DC}.

The time domain step response of the buck converter is tested. Being the electronic load configured in constant voltage mode, the PV source emulator applies steps to the current reference. Experimental results are shown in Figure 9 for different operating areas: high current–low voltage, low current–high voltage, and high current–high voltage. The figure shows how the inductor current (I_{out}) can be used to control the PV emulated current (I_{PV}) and justifies the use of an output DC-capacitor (that of the LC filter) as it absorbs the high-frequency current ripple produced by the switching converter.

If the reference voltage of the programmable electronic load, which agrees with the emulator output voltage, is varied along the whole output voltage range of the electronic load (minimum voltage: 7 V) for different irradiance levels and for different temperatures, it can be observed that the output current fits the curves of the programmed PV source (Figures 10 and 11). The plotted curves in these figures is obtained from the voltage–current data provided by the datasheet of the PV module. Note that the lowest voltage of the experimental data is limited by the electronic load.

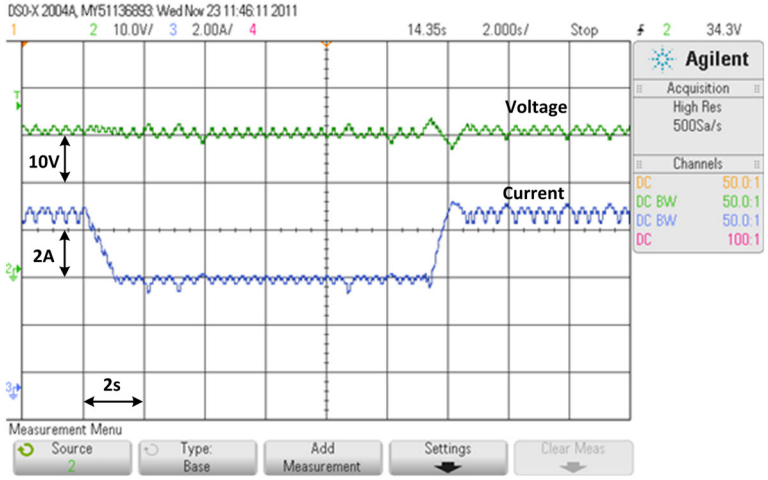

Figure 22. Maximum power point tracking evolution under irradiance steps from 1000 to 600 W/m^{2}and back to 1000 W/m^2. Transition time is 1 s. The ambient temperature is 25 °C.

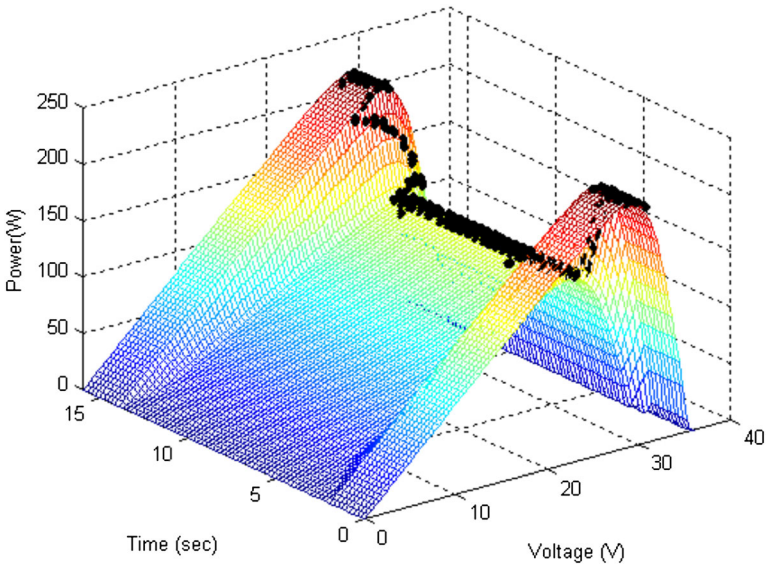

Figure 23. Irradiance steps from 1000 to 600 W/m^2 plotted over the power–voltage surface. Transition time is 1 s. The ambient temperature is 25 °C. Dots represent the maximum power point tracking evolution.

To test the performance of the emulator under dynamic irradiance changes the programmable electronic load is configured in constant voltage mode. Then, an irradiance step is emulated. The irradiance steps applied are of 200 W/m^2 with a falling time of 4 s. This test is carried out at different voltages: constant current region (15 V), near the MPP (28 V), and constant voltage region (32 V). Oscilloscope captures for these irradiance steps are shown in Figures 12–14. To check if the captured output voltage and output current fits the curves of the emulated PV source, a three-dimensional plot with the *I–V* and *P–V* curves is shown in Figure 15. The plotted surface represents the data current–voltage irradiance of the curves introduced in the microcontroller. The dots represent the data captured with the oscilloscope for 15, 28, and 32 V.

In the next test of the PV emulator, the prototype is connected to a grid-connected single-phase microinverter of 230 W output power. The microinverter is a cascaded double stage topology (DC/DC followed by DC/AC converter), whose control loops are designed to regulate its input DC voltage and the grid injected current [3]. The microinverter MPPT algorithm varies the reference of its input voltage (i.e., the emulator output voltage) to track the MPP of the PV source, that is, the PV emulator in this test. The algorithm used is the classical Perturb and Observe [21], updated at 50 Hz with a voltage step of 1 V. The energy obtained from the PV emulator is injected into the grid

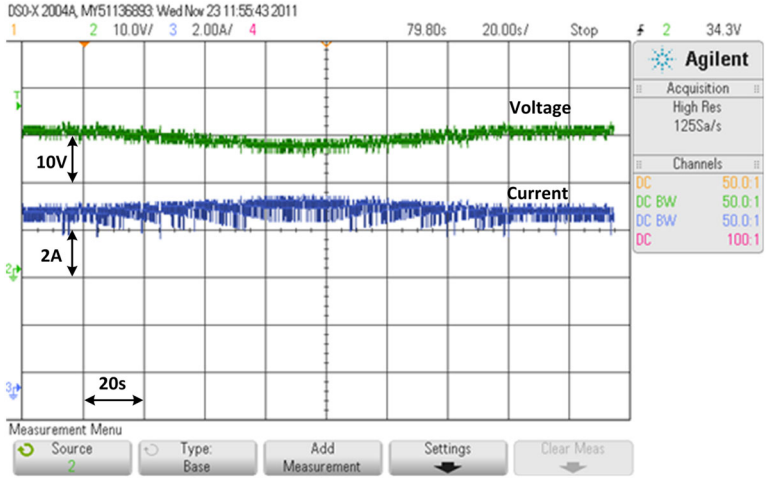

Figure 24. Maximum power point tracking evolution under temperature change from 25 to 55 °C and back to 25 °C in 60 s. The emulated irradiance is 1000 W/m^2.

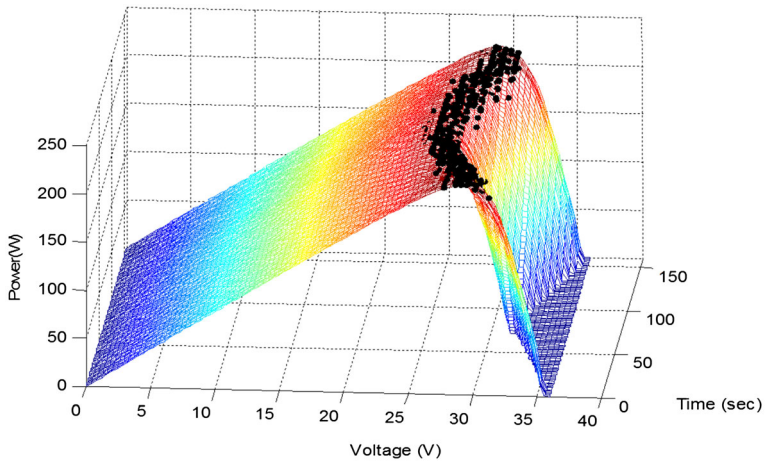

Figure 25. Temperature change from 25 to 55 °C and back to 25 °C in 60 s plotted over the power–voltage curve. Dots represent the maximum power point tracking evolution.

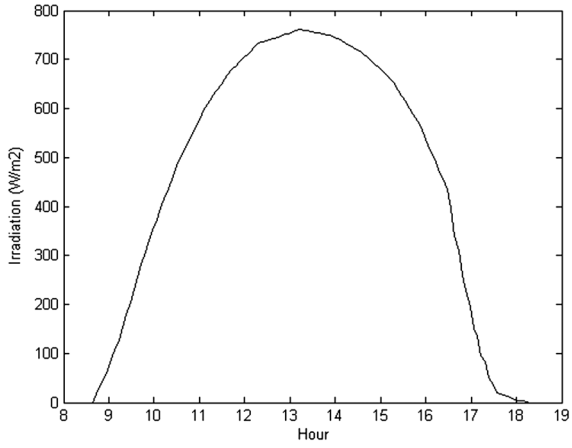

Figure 26. Evolution of the irradiance level during one day (January).

by means of the microinverter (Figure 16), whose characteristics are summarized in Table III.

The PV emulator is used for the characterization of the MPPT performance of the microinverter at the following operating conditions of the emulated PV source: 1000 W/m^2 and 25 °C. Under these conditions, the MPP is $V_{PV\_MPP} = 28.9$ V, $I_{PV\_MPP} = 7.5$ A. The voltage and current provided by the emulator, V_{PV} and I_{PV}, are shown in Figure 17. It can be observed that by the action of the MPPT algorithm, the microinverter input voltage, V_{PV}, is varied to track the MPP of the emulated PV source.

In the *I–V* curve of any real PV source, it holds that the absolute value of the negative slope is lower at the left side of the MPP than at the right side of the MPP. Therefore, when the MPPT algorithm produces negative voltage steps of V_{PV} that push this voltage below V_{PV_MPP}, positive current steps of decreasing size are observed. This dynamic behavior

Prog. Photovolt: Res. Appl. 2014; **22**:227–241 © 2012 John Wiley & Sons, Ltd.
DOI: 10.1002/pip

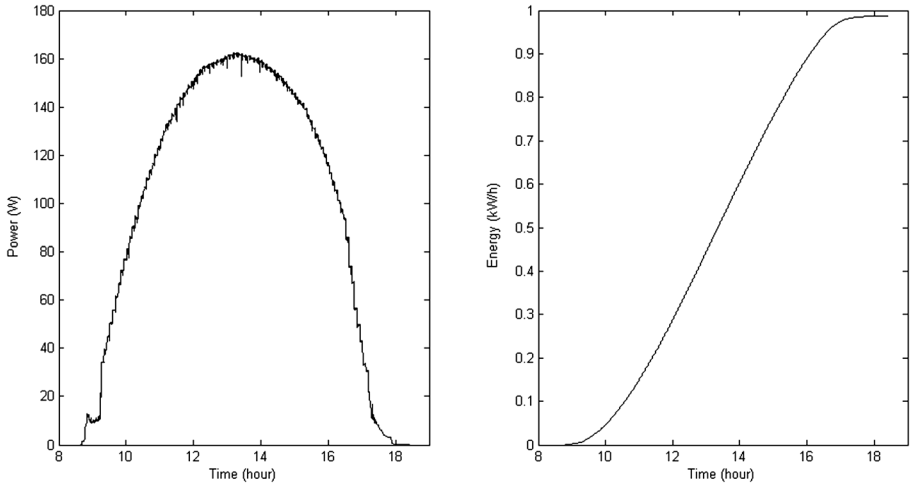

Figure 27. Power and energy during one day obtained from the photovoltaic emulator feeding the microinverter.

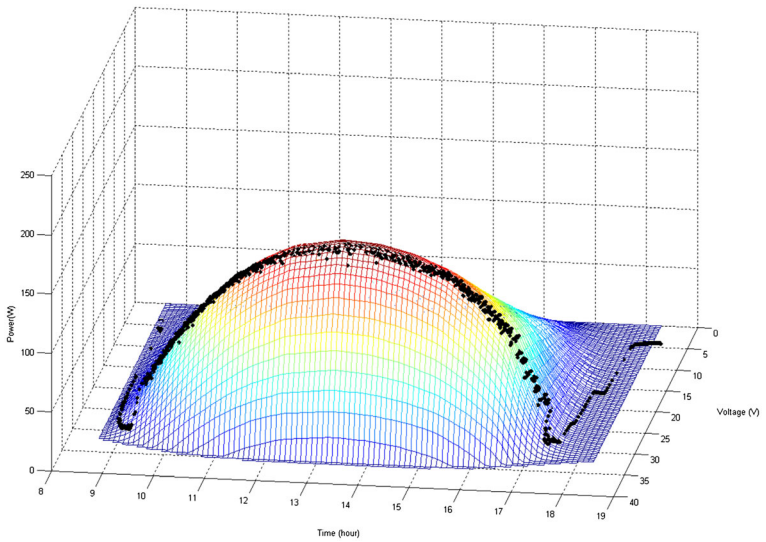

Figure 28. Power over one day plotted over the power–voltage surface.

is reproduced by the emulator when it feeds the microinverter, as it is shown in Figure 18.

The quality of the MPPT algorithm strongly depends on the minimum voltage step size of V_{PV} that can be applied in each iteration [22]. The smaller this step size, the smaller are the dynamic deviations from the PV source MPP, which allows a better extraction of the available PV energy over time. The emulator presented in this paper is able to respond to 100 mV voltage steps, as it is shown in Figure 19. The emulator responds to steps lower than the 0.25% of its full scale.

Another parameter to characterize the quality of the MPPT algorithm is the response to transients of the PV source irradiance or temperature. Three different transient responses have been tested with the emulator feeding the microinverter, which is running the MPPT algorithm: a slow, 10 s, transient of the irradiance (Figures 20 and 21), a fast, 1 s, transient of the irradiance (Figures 22 and 23), and a temperature transient (Figures 24 and 25). Note that V_{PV_MPP} varies very slightly (from 28.9 to 28.4 V) to the irradiance steps shown in Figure 20 so that its variation is almost imperceptible at the vertical scale of the oscilloscope. These figures show that the emulator can be used to evaluate the performance of the MPPT algorithm of a microinverter under these transient conditions.

When testing the performance of MPPT algorithms, it is a usual practice to test the power converter for a long period, emulating irradiance variations during one day. It is possible to program inside the microcontroller a curve similar to that shown in Figure 26, which represents the irradiance level during one sunny day of winter [6].

The MPPT algorithm of the microinverter is tested with the PV emulator connected at its input. The power and energy obtained from the emulator are shown in Figure 27.

The output power plotted over the power–voltage curve is shown in Figure 28.

5. CONCLUSIONS

To characterize and evaluate PV electronic power converters and facilities, it is necessary to provide a power source that emulates the current–voltage characteristics of a PV source. An emulator can simulate every weather or temperature condition and PV modules of different manufacturers. The tests can be repeated in the same conditions easily.

Commercial PV emulators present several drawbacks, as a high cost and the impossibility of emulating rapidly changing atmospheric conditions. In this paper, a buck DC–DC converter topology is selected as PV emulator because it is efficient and inexpensive. The 3 kW PV emulator presented has been designed to have a current-loop bandwidth of 10 kHz, much higher than the iteration speed of the usual MPPT algorithms of any PV converter under test. The control architecture is based on an analog average current loop and a voltage-to-current lookup table. The volume of the emulator is 1.7 dm^3 and its weight around 3 kg. The production cost of this emulator could be lower than $210.

An emulator prototype has been validated by means of simulation and experimental results. It has been demonstrated that the output current–voltage and voltage–power characteristics match the preprogrammed curves of the PV source. The prototype can emulate changes of irradiance and temperature with different dynamics. Finally, a grid-connected microinverter has been tested, showing how this inexpensive emulator can help to evaluate the performance of MPPT algorithms, both in fast transient conditions and in the long term.

Summing up, the emulator proposed in this paper presents a low-cost alternative to emulate the operation of PV sources and power converters in a laboratory under different operating conditions.

ACKNOWLEDGEMENT

This work is supported by the Spanish Ministry of Science and Innovation under grant ENE2009-13998-C02-02.

REFERENCES

1. Prapanavarat C, Barnes M, Jenkins N. Investigation of the performance of a photovoltaic AC module. *IEEE Proceedings - Generation, Transmission and Distribution* 2002; **149**(4): 472–478. DOI: 10.1049/ip–gtd:20020141
2. Durán E, Andújar JM, Galán J, Sidrach-de-Cardona M. Methodology and experimental system for measuring and displaying I−V characteristic curves of PV facilities. *Progress in Photovoltaics: Research and Applications* 2009; **17**(8): 574–586. DOI: 10.1002/pip.909
3. Garcerá G, González-Medina R, Figueres E, Sandia J. Dynamic modeling of DC−DC converters with peak current control in double-stage photovoltaic grid-connected inverters. *International Journal of Circuit Theory and Applications*. Available on-line, 2011. DOI: 10.1002/cta.756
4. Piliougine M, Carretero J, Mora-López L, Sidrach-de-Cardona M. Experimental system for current–voltage curve measurement of photovoltaic modules under outdoor conditions. *Progress in Photovoltaics: Research and Applications* 2011; **19**(5): 591–602. DOI: 10.1002/pip.1073
5. Camino-Villacorta M, Egido-Aguilera MA, Díaz P. Test procedures for maximum power point tracking charge controllers characterization. *Progress in Photovoltaics: Research and Applications* 2011. DOI: 10.1002/pip.1139
6. Sanchis P, López J, Ursúa A, Gubía E, Marroyo L.On the testing, characterization, and evaluation of PV inverters and dynamic MPPT performance under real varying operating conditions. *Progress in Photovoltaics: Research and Applications* 2007; **15**(6): 541–556. DOI: 10.1002/pip.763
7. Dolan D, Durago J, Crowfoot J, Taufik. Simulation of a photovoltaic emulator. *North American Power Symposium (NAPS)* 2010; 1–7. DOI: 10.1109/NAPS.2010.5618941
8. Kjaer SB, Pedersen JK, Blaabjerg F. A review of single-phase grid-connected inverters for photovoltaic modules. *IEEE Transactions on Industry Applications* 2005; **41**(5): 1292–1306. DOI: 10.1109/TIA.2005.853371
9. Meneses D, Garcia O, Alou P, Oliver JA, Prieto R, Cobos JA. Single-stage grid-connected forward microinverter with boundary mode control, *Energy Conversion Congress and Exposition (ECCE)* 2011; 2475–2480. DOI: 10.1109/ECCE.2011.6064097
10. Kondrath N, Kazimierczuk MK. Comparison of wide- and high-frequency duty-ratio-to-inductor-current transfer functions of DC-DC PWM buck converter in CCM. *IEEE Transactions on Industrial Electronics* 2012; **59**(1): 641–643. DOI: 10.1109/TIE.2011.2134053
11. Yun TT, Kirschen DS, Jenkins N. A model of PV generation suitable for stability analysis. *IEEE Transactions on Energy Conversion* 2004; **19**(4): 748–755. DOI: 10.1109/TEC.2004.827707
12. Mäki A, Valkealahti S, Leppäaho J. Operation of series-connected silicon-based photovoltaic modules under partial shading conditions. *Progress in Photovoltaics: Research and Applications* 2011; DOI: 10.1002/pip.1138
13. Villalva MG, Gazoli JR, Filho ER. Comprehensive approach to modeling and simulation of photovoltaic arrays. *IEEE Transactions on Power Electronics* 2009; **24**(5): 1198–1208. DOI: 10.1109/TPEL.2009.2013862

14. Shengyi L, Dougal RA. Dynamic multiphysics model for solar array. *IEEE Transactions on Energy Conversion* 2002; **17**(2): 285–294. DOI: 10.1109/TEC.2002.1009482.
15. Koran A, Sano K, Rae-Young K, Jih-Sheng L. Design of a photovoltaic simulator with a novel reference signal generator and two-stage LC output filter, *Energy Conversion Congress and Exposition, 2009. ECCE 2009. IEEE* 2009; 319–326. DOI: 10.1109/ECCE.2009.5316190
16. Orduz R, Solórzano J, Egido MÁ, Román E. Analytical study and evaluation results of power optimizers for distributed power conditioning in photovoltaic arrays. *Progress in Photovoltaics: Research and Applications* 2011; n/a. DOI: 10.1002/pip.1188.
17. Mekki H, Mellit A, Kalogirou SA, Messai A, Furlan G. FPGA-based implementation of a real time photovoltaic module simulator. *Progress in Photovoltaics: Research and Applications* 2010; **18**(2): 115–127. DOI: 10.1002/pip.950
18. Mohan N, Undeland T, Robbins W. Power electronics: converters, applications and design (3rd edn). 2003.
19. Garcera G, Figueres E, Pascual M, Benavent JM. Robust model following control of parallel buck converters. *IEEE Transactions on Aerospace and Electronic Systems* 2004; **40**(3): 983–997. DOI: 10.1109/TAES.2004.1337469
20. Vorperian V. Simplified analysis of PWM converters using model of PWM switch. Continuous conduction mode. *IEEE Transactions on Aerospace and Electronic Systems* 1990; **26**(3): 490–496. DOI: 10.1109/7.106126.
21. Packiam P, Jain NK, Singh IP. Microcontroller-based simple maximum power point tracking controller for single-stage solar stand-alone water pumping system. *Progress in Photovoltaics: Research and Applications* 2011; DOI: 10.1002/pip.1207.
22. Chuanzong F, Shiping S. Simulation studying of MPPT control by a new method for photovoltaic power system. *Electrical and Control Engineering (ICECE), 2011 International Conference on* 2011,1274–1278. DOI: 10.1109/ICECENG.2011.6057918